Journal of Thermal Analysis and Calorimetry, Vol. 71 (2003) 567–582

COMPARATIVE THERMODYNAMIC STUDY OF GaSb–Sn SYSTEM

D. Živković[1*], *I. Katayama*[2], *A. Kostov*[3] *and Ž. Živković*[1]

[1]University of Belgrade, Technical Faculty, VJ 12, 19210 Bor, Yugoslavia
[2]Osaka University, Graduate School of Engineering, Department of Material Science and Processing, 2-1, Yamadaoka, Suita, Osaka 565-0871, Japan
[3]Copper Institute, Zeleni bulevar 35, 19210 Bor, Yugoslavia

(Received June 10, 2002; in revised form July 24, 2002)

Abstract

The results of comparative thermodynamic study of GaSb–Sn system are presented in this paper. Calorimetric measurements according to Oelsen's method and EMF measurements with zirconia as solid electrolyte were used for experimental investigation, while Chou's general solution model, Toop, Kohler and Muggianu methods were used for predicting thermodynamic characteristics in this system. Also, phase diagram of this quasibinary system, determined by DTA and optical microscopy, is presented.

Keywords: Ga–Sb–Sn alloys, ternary systems, thermodynamics

Introduction

Many investigations were done in order to give the correct interpretation of the phenomena occurring in alloy systems containing semiconducting compounds. Thermodynamic study of these materials is important from scientific and technological point of view, since ternary and multicomponent systems are not completely experimentally investigated, although some of the binary systems have been studied extensively.

For their important industrial application in the solid-state electronic devices, GaSb-based ternary alloys with Bi, Ge, In, Sn, Te, S, have been the subject of an increasing attention in the semiconductor production [1–6]. Ternary system Ga–Sb–Sn is one of these systems.

There are a lot of literature data concerning the thermodynamics of its constituent binary systems Ga–Sb [7–13], Sb–Sn [14] and Sn–Ga [15–18]. But, there is only one reference on thermodynamics of ternary Ga–Sb–Sn system by Katayama and collaborators [19], in which activities of gallium, in liquid Ga–Sb–Sn alloys along three lines of constant molar ratio of Sb:Sn, were measured by EMF method using zirconia as solid electrolyte.

* Author for correspondence:jmm@eunet.yu

1388–6150/2003/ $ 20.00
Akadémiai Kiadó, Budapest

Considering the phase equilibrium investigations, Osamura and Murakami [20] suggested the phase diagram of Ga–Sb–Sn ternary system, while Gerdes and Predel [21] researched quasibinary section GaSb–Sn in this system.

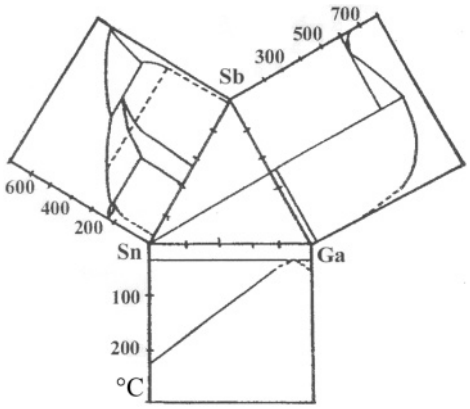

Fig. 1 Ternary system Ga–Sb–Sn with signed quasibinary section GaSb–Sn

In order to contribute to the better knowledge of the Ga–Sb–Sn system thermodynamics, the results of comparative thermodynamic analysis (experimental and thermodynamic predicting) and phase diagram investigations of the quasibinary section GaSb–Sn (shown in Fig. 1) are presented in this paper.

Experimental

Oelsen calorimetry and EMF measurements with zirconia as solid electrolyte has been performed in the experimental part of thermodynamic investigation in this paper, while DTA and optic microscopy were used for phase diagram determination.

All experiments were performed using metals Ga, Sb, Sn of p.a. purity.

Oelsen calorimetry

Measurements were carried out according to procedure described in [5, 22–24], in an air atmosphere. Water equivalent was determined by a standard method using dissolved Na_2CO_3, and its value was 3870 J K^{-1}. Compositions and masses of the investigated alloys are presented in Table 1. Alloy volume was constant 0.1 cm^3.

EMF measurements

EMF method with zirconia as solid electrolyte has been used. Experimental equipment and procedure is presented in [19]. EMFs of cell

$$(-)W, Ga, Ga_2O_3 \,|\, ZrO_2\ (+Y_2O_3) \,|\, Sn_x(Ga_{0.5}Sb_{0.5})_{1-x}\ (l), Ga_2O_3, W(+) \qquad (I)$$

Table 1 Composition and masses of the investigated samples

Alloy	x_{Sn}	x_{Ga}	x_{Sb}	Mass% Sn	Mass% Ga	Mass% Sb	Mass/g	m_{Sn}	m_{Ga}	m_{Sb}
L0	0	0.5	0.5	0	36.41302	63.58698	0.637744	0	0.232222	0.405522
L1	0.1	0.45	0.45	12.10746	32.00433	55.88822	0.647654	0.078414	0.207277	0.361962
L2	0.2	0.4	0.4	23.66087	27.79738	48.54175	0.657402	0.155547	0.182741	0.319114
L3	0.3	0.35	0.35	34.69741	23.77864	41.52395	0.666992	0.231429	0.158602	0.276961
L4	0.4	0.3	0.3	45.25101	19.93576	34.81323	0.676427	0.30609	0.134851	0.235486
L5	0.5	0.25	0.25	55.35269	16.25743	28.38988	0.685712	0.37956	0.111479	0.194673
L6	0.6	0.2	0.2	65.03087	12.73332	22.23582	0.69485	0.451867	0.088477	0.154506
L7	0.7	0.15	0.15	74.31163	9.353911	16.33446	0.703845	0.523038	0.065837	0.114969
L8	0.8	0.1	0.1	83.21896	6.110483	10.67056	0.712699	0.593101	0.043549	0.076049
L9	0.9	0.05	0.05	91.77496	2.994987	5.230058	0.721416	0.66208	0.021606	0.03773
L10	1	0	0	100	0	0	0.73	0.73	0	0

were measured. Ga_2O_3 powder was added to the alloy electrode and referent electrode in a mass ratio 1:9. Zirconia solid electrolyte crucibles ($0.92ZrO_2+0.08Y_2O_3$), dimension 8×5×50 mm, were used. EMFs of cell and the cell temperature were measured with digital voltmeter (Multi Logging Meter AD-5311, A&D) with printer. Temperature was controlled using Pt–13RhPt thermocouple and a thermocontroler. All experiments were carried out under argon atmosphere. Compositions of the investigated alloys were as follows: x_{Sn}=0, 0.052, 0.176, 0.335, 0.539, 0.7, 0.8, 0.9.

Differential thermal analysis

A MOM Derivatograph, Hungary was used in the experimental work. DTA curves have been recorded at heating rate of 10°C min^{-1} in an air atmosphere, while Al_2O_3 was used as a reference material during measurements. In this case, the following compositions of the investigated alloys were used: x_{Sn}=0, 0.1, 0.2, 0.3, 0.4, 0.5, 0.6, 0.7, 0.8, 0.9, 1.

Optical microscopy

A Reichert MeF2 microscope was used. Solution of (8 mL H_2SO_4+2 g $K_2Cr_2O_7$) was used as etching reactant.

Theoretical principles

Different methods of thermodynamic predicting, such as Chou's general solution model [25], Toop [27], Kohler [28] and Muggianu model [29], were used for analytical determination of thermodynamic properties in Ga–Sb–Sn system.

The basic theoretical interpretations of these models are given:

Chou's general solution model [25, 26]

$$G^{E}=\Delta G^{E}_{12}\frac{X_1X_2}{(X_1+\xi_{12}X_3)(X_2+(1-\xi_{12})X_3)}+\Delta G^{E}_{31}\frac{X_1X_3}{(X_3+\xi_{31}X_2)(X_1+(1-\xi_{31})X_2)}+ \\ +\Delta G^{E}_{23}\frac{X_3X_2}{(X_2+\xi_{23}X_1)(X_3+(1-\xi_{23})X_1)} \quad (1)$$

where are $X_{1(12)}=x_1+x_3\xi_{12}$; $X_{3(31)}=x_3+x_2\xi_{31}$; $X_{2(23)}=x_2+x_1\xi_{23}$ and ξ_{ij} is the similarity coefficient.

Toop model [27]

$$G^{E}=\frac{x_2}{1-x_1}\Delta G^{E}_{12}(x_1;1-x_1)+\frac{x_3}{1-x_1}\Delta G^{E}_{13}(x_1;1-x_1)+ \\ +(x_2+x_3)^2\Delta G^{E}_{23}\left(\frac{x_2}{x_2+x_3};\frac{x_3}{x_2+x_3}\right) \quad (2)$$

Kohler model [28]

$$G^{E}=(x_1+x_2)^2\,\Delta G^{E}_{12}\left(\frac{x_1}{x_1+x_2};\frac{x_2}{x_1+x_2}\right)+$$
$$+(x_2+x_3)^2\,\Delta G^{E}_{23}\left(\frac{x_2}{x_2+x_3};\frac{x_3}{x_2+x_3}\right)+ \quad (3)$$
$$+(x_3+x_1)^2\,\Delta G^{E}_{31}\left(\frac{x_{31}}{x_1+x_3};\frac{x_1}{x_1+x_3}\right)$$

Muggianu model [29]

$$G^{E}=\frac{4x_1x_2}{(1+x_1-x_2)(1+x_2-x_1)}\Delta G^{E}_{12}\left(\frac{1+x_1-x_2}{2};\frac{1+x_2-x_1}{2}\right)+$$
$$+\frac{4x_2x_3}{(1+x_2-x_3)(1+x_3-x_2)}\Delta G^{E}_{23}\left(\frac{1+x_2-x_3}{2};\frac{1+x_3-x_2}{2}\right)+ \quad (4)$$
$$+\frac{4x_3x_1}{(1+x_3-x_1)(1+x_1-x_3)}\Delta G^{E}_{31}\left(\frac{1+x_3-x_1}{2};\frac{1+x_1-x_3}{2}\right)$$

Hillert model [30]

$$G^{E}=\frac{x_2}{1-x_1}\Delta G^{E}_{12}(x_1;1-x_1)+\frac{x_3}{1-x_1}\Delta G^{E}_{13}(x_1;1-x_1)+\frac{x_2x_3}{v_{23}v_{32}}\Delta G^{E}_{23}(v_{23};v_{32}) \quad (5)$$

where is $v_{ij}=1/2(1+x_i-x_j)$.

In all given equations, G^{E} and ΔG^{E}_{ij} correspond to the integral molar excess Gibbs energies for ternary and binary systems, respectively, while x_1, x_2, x_3 correspond to the mole fraction of components in investigated ternary system.

Results and discussion

Oelsen's calorimetry

Based on the cooling curves obtained by Oelsen's calorimetry, the temperature changes of the calorimeter used were determined for all samples in the investigated temperature interval 300–1100 K. That enabled the determination of the dependence of the calorimeter temperature change on the composition and temperature, and the construction of the enthalpy isotherm diagram for the investigated temperature interval 300–1100 K, presented in Fig. 2.

Following the basic equation in Oelsen's thermodynamic analysis [5, 22–24], in the case of investigated GaSb–Sn system given as

$$-\frac{G_{\mathrm{Sn}}^{\mathrm{M}}}{T}=\int_{1/T_0}^{1/T} H_{\mathrm{x,T}}\mathrm{d}\left(\frac{1}{T}\right)=-R\ln a_{\mathrm{Sn}} \tag{6}$$

(where $G_{\mathrm{Sn}}^{\mathrm{M}}$ – is the partial molar Gibbs energy for tin, T_0 – is the starting temperature, T – is the final temperature, $H_{\mathrm{x,T}}$ – is the enthalpy value measured in the Oelsen calorimeter for the temperature change from T_0 to T, R – is the gas constant and a_{Sn} – is the activity of tin), further calculations in the thermodynamic analysis was done. Based on Eq. (5) and the results of graphic planimetry, the tangents were constructed for the calculation of $-R\ln a_{\mathrm{Sn}}$ at temperatures 1000, 1050 and 1100 K, which enabled the determination of tin activities, activity coefficients and partial molar quantities. The results are given in Table 2.

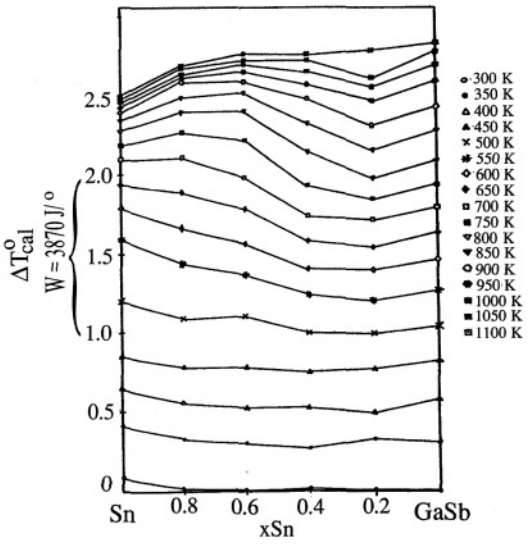

Fig. 2 The enthalpy isotherm diagram for the temperature interval 300–1100 K

Slight positive deviation from the ideal behavior can be noticed for tin activities in the whole composition range for all investigated temperatures, while a slight change of tin activities with temperature is present. Negative values for partial molar Gibbs energies of mixing and positive values for partial molar excess Gibbs energies are typical for all investigated alloys and complete temperature range.

EMF measurements with zirconia as solid electrolyte

After the cell temperature reached the desired value, it was held constant for ca 12 h, and then tungsten lead wire was dipped into the alloy electrode. Thereafter, it took about several tens of minutes to several hours to reach stable *EMF* of the cell. On changing the temperature, equilibration at a new temperature took a very short period of time. The tungsten lead wire could be used to stir the alloy electrode to confirm the equilibrium *EMF*.

Table 2 Results of the Oelsen's quantitative thermodynamic analysis at 1000, 1050 and 1100 K (energies in J mol^{-1})

T/K	1000				1050				1100			
x_{Sn}	a_{Sn}	γ_{Sn}	G^{M}_{Sn}	G^{E}_{Sn}	a_{Sn}	γ_{Sn}	G^{M}_{Sn}	G^{E}_{Sn}	a_{Sn}	γ_{Sn}	G^{M}_{Sn}	G^{E}_{Sn}
0.1	0.107	1.067	–18581	539.17	0.105	1.048	–19675	409.28	0.102	1.025	–20877	225.82
0.2	0.22	1.098	–12588	777.28	0.212	1.059	–13541	500.43	0.204	1.022	–14538	199.02
0.3	0.311	1.038	–9710	310.08	0.308	1.025	–10281	215.56	0.306	1.019	–10830	172.13
0.4	0.412	1.028	–7372	229.59	0.413	1.033	–7720	283.43	0.405	1.012	–8266	109.09
0.5	0.516	1.032	–5501	261.88	0.513	1.026	–5827	224.07	0.507	1.014	–6212	127.15
0.6	0.607	1.012	–4151	99.174	0.618	1.03	–4201	258.04	0.614	1.024	–4461	216.9
0.7	0.714	1.02	–2801	164.64	0.71	1.014	–2990	121.37	0.714	1.02	–3081	181.1
0.8	0.82	1.025	–1650	205.29	0.805	1.007	–1894	60.895	0.815	1.019	–1871	172.13
0.9	0.908	1.009	–802.4	74.491	0.914	1.015	–785	129.97	0.919	1.021	–772.5	190.06

Table 3 Temperature dependence of *EMF* of cell (I) and thermodynamic quantities of gallium obtained at 1000, 1050 and 1100 K in GaSb–Sn system

x_{Sn}	E/mV	T/K	a_{Ga}	γ_{Ga}	G^{E}_{Ga}/J mol^{-1}
0	$-4.86+32.48\cdot10^{-3}T$/K±3.83	1000	0.382	0.762	–2236
		1050	0.379	0.758	–2414
		1100	0.376	0.753	–2599
0.052	$7.58+22.69\cdot10^{-3}T$/K±3.10	1000	0.348	0.753	–2557
		1050	0.353	0.745	–2575
		1100	0.357	0.753	–2595
0.176	$7.01+24.91\cdot10^{-3}T$/K±3.53	1000	0.329	0.799	–1870
		1050	0.333	0.808	–1863
		1100	0.336	0.817	–1854
0.335	$9.81+24.73\cdot10^{-3}T$/K±3.19	1000	0.300	0.902	–859
		1050	0.305	0.917	–761
		1100	0.310	0.930	–660
0.539	$-21.24+60.94\cdot10^{-3}T$/K±7.61	1000	0.251	1.086	672
		1050	0.242	1.048	404
		1100	0.235	1.016	138
0.700	$1.69+47.85\cdot10^{-3}T$/K±3.89	1000	0.178	1.187	1427
		1050	0.179	1.191	1523
		1100	0.179	1.193	1616
0.800	$-25.85+84.70\cdot10^{-3}T$/K±3.48	1000	0.129	1.288	2103
		1050	0.123	1.234	1833
		1100	0.119	1.187	1565
0.900	$-24.65+10.29\cdot10^{-3}T$/K±11.34	1000	0.0655	1.311	2249
		1050	0.0629	1.258	2003
		1100	0.0606	1.212	1760

The experimental results are shown in Fig. 3. As all the data points distribute around a straight line for each composition, the relations between *EMF* (E mV) and temperature (T/K) are obtained by least-square regression analysis, and are listed in Table 3.

For tin concentrations higher than 0.335, gallium activities show negative deviation from Raoult law, while for lower tin concentrations, slight positive deviation of gallium activities from the ideal behavior is present.

Thermodynamic predicting

Basic thermodynamic data on the constituent binary subsystems Ga–Sb, Sb–Sn and Sn–Ga, needed for predicting of thermodynamic properties in the investigated GaSb–Sn system, are fitted to the Redlich–Kister presentation by Eq. (7):

$$\Delta G^{E}_{ij}=x_i x_j \sum (x_i-x_j)^{\upsilon} L_{ij}^{(\upsilon)}(T)$$
$$L_{ij}^{(\upsilon)}(T)=a_{ij}^{(\upsilon)}+b_{ij}^{(\upsilon)}T \qquad (7)$$

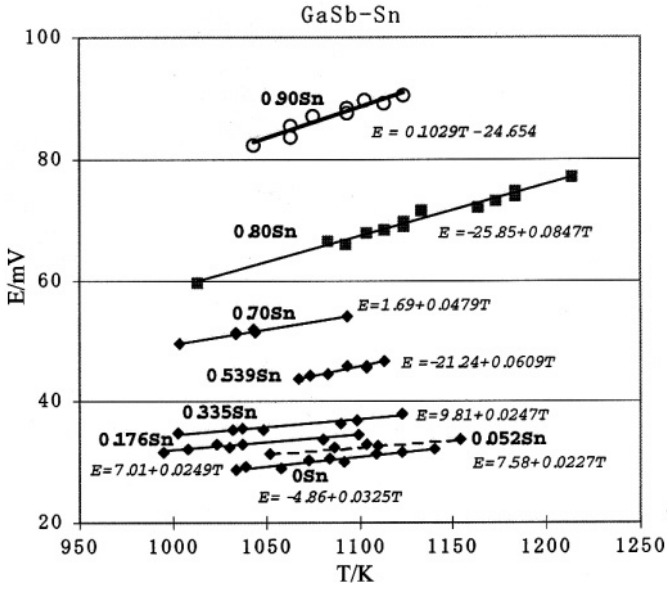

Fig. 3 Temperature dependence of the *EMF* of cell (I)

According to the experimental data in [7, 14, 15], ΔG_{ij}^{E} values were calculated in the temperature range of 1000–1200 K at intervals of 50 K. The fitting parameters were obtained and shown in Table 4, as well as similarity coefficients determined as important parameters in general solution model application.

Based on these starting data, calculations were carried out according to different predicting methods for all alloys in the investigated GaSb–Sn system at different temperatures of 1000, 1050 and 1100 K. The results of thermodynamic predictions, according to Chou's general solution model [25, 26] and models of Toop [27], Kohler [28], Muggianu [29] and Hillert [30], are given in Table 5. Good mutual agreement could be noticed between the results of different applied thermodynamic predicting models.

Table 4 Redlich–Kister parameters for ΔG_{ij}^{E} and similarity coefficients for Ga–Sb, Sb–Sn and Sn–Ga systems

System	ν	$a_{ij}^{(\nu)}$	$b_{ij}^{(\nu)}$	Temp. range/K	System	*T*/K	ξ_{ij}
	0	–832.80	–6.6885			1000	0.987
Ga–Sb	1	5598.30	–6.6301	1000–1200	Ga–Sb	1050	0.980
	2	–120.56	–1.1081			1100	0.972
	0	16792	–12.1380			1000	0.443
Sn–Ga	1	–15241	13.0650	1000–1200	Sn–Ga	1050	0.429
	2	5651.50	–5.2132			1100	0.415
	0	–4855.5	–1.6688			1000	0.016
Sb–Sn	1	1092.70	–1.1787	1000–1200	Sb–Sn	1050	0.026
	2	1752.80	–0.7129			1100	0.039

Table 5 Integral molar excess Gibbs energies for GaSb–Sn system at 1000, 1050 and 1100 K calculated by different predicting methods (energies in J mol^{-1})

Alloy	Chou	Toop	Hillert	Kohler	Muggianu
			1000 K		
x_{Sn}			ΔG^E/J mol^{-1}		
0.1	–1587	–1613	–1367	–1658	–1645
0.2	–1344	–1351	–922	–1407	–1388
0.3	–1135	–1089	–564	–1137	–1128
0.4	–948	–835	–293	–861	–872
0.5	–774	–595	–104	–602	–628
0.6	–607	–375	12	–370	–405
0.7	–444	–184	77	–174	–212
0.8	–285	–28	90	–19	–58
0.9	–135	84	94	89	48
			1050 K		
x_{Sn}			ΔG^E/J mol^{-1}		
0.1	–1704	–1722	–1473	–1741	–1735
0.2	–1474	–1482	–1048	–1499	–1488
0.3	–1264	–1239	–707	–1244	–1239
0.4	–1065	–997	–447	–988	–996
0.5	–872	–763	–264	–743	–761
0.6	–683	–539	–144	–516	–540
0.7	–498	–334	–74	–312	–340
0.8	–318	–153	–30	–137	–167
0.9	–150	–0.321	12	7	–25
			1100 K		
x_{Sn}			ΔG^E/J mol^{-1}		
0.1	–1651	–1830	–1579	–1825	–1825
0.2	–1539	–1612	–1174	–1592	–1587
0.3	–1427	–1388	–849	–1353	–1352
0.4	–1315	–1159	–601	–1116	–1119
0.5	–1204	–930	–423	–884	–893
0.6	–1092	–704	–301	–661	–675
0.7	–980	–485	–218	–451	–468
0.8	–868	–277	–151	–255	–275
0.9	–757	–85	–71	–75	–99

Comparative thermodynamic study

In order to compare the results of the thermodynamic predicting with obtained experimental data at investigated temperatures, partial thermodynamic quantities for tin and gallium were derived according to well known expressions: $G_i^E = G^E + (1-x_1)(\partial G^E/\partial x_i) = RT\ln\gamma_i$ and $a_i = x_i\gamma_i$. The results of calculation, which include tin and gallium activities for the researched alloys, are shown in Table 6.

The graphic presentation of the comparison with experimental data, at temperature of 1000 K, is given in Fig. 4.

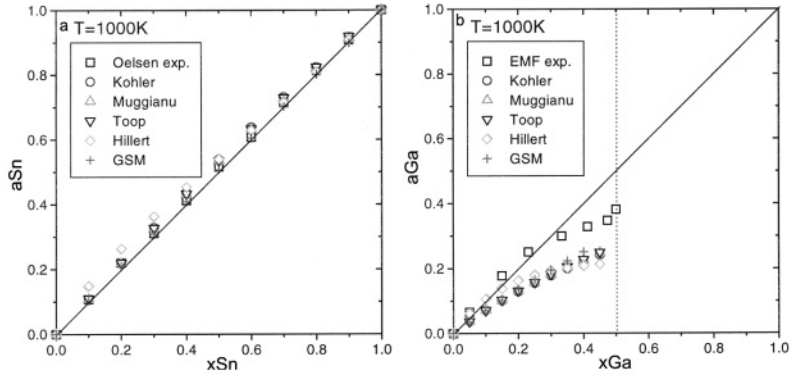

Fig. 4 Comparison between experimental and predicted results for the dependence a_{Sn}; a – and a_{Ga}; b – *vs*. molar content at 1000 K

Good agreement between experimental thermodynamic data on tin activities, obtained by Oelsen calorimetry and thermodynamic predicting, is noticed. Considering the thermodynamic behavior of gallium in the investigated alloys in Ga–Sb–Sn system, slight deviation of experimental data is shown, comparing to predicted thermodynamic values.

Phase diagram determination

The phase diagram of the Ga–Sb–Sn system was investigated based on the cooling curves obtained by the Oelsen's calorimetry, DTA results and the results of microstructure analysis.

DTA results are shown in Fig. 5, while characteristic microphotograph recorded by optical microscopy for the sample L6 (with x_{Sn}=0.6) is presented in Fig. 6.

Graphical representation of the obtained phase diagram for GaSb–Sn system, compared with literature data [20, 21], is given in Fig. 7.

The eutectic type of the phase diagram is noticed. The quasibinary hypoeutectic alloys, presented in the widest part of the investigated concentration range in the GaSb–Sn system, solidify with the primary crystallization of the intermetallic compound GaSb and the eutectic reaction /GaSb+Sn/ (dark phase). According to the results of optical microscopy, quantity of the primarily solidified GaSb crystals (light phase) increases by decreasing of tin concentration.

Table 6 The values for tin and gallium activities at investigated temperatures calculated from the predicted results

Alloy	Chou	Toop	Hillert	Kohler	Muggianu	Chou	Toop	Hillert	Kohler	Muggianu
	1000 K									
x_{Sn}	a_{Sn}					a_{Ga}				
0.1	0.105	0.108	0.109	0.108	0.148	0.277	0.249	0.213	0.242	0.247
0.2	0.209	0.218	0.219	0.217	0.264	0.251	0.227	0.209	0.221	0.225
0.3	0.31	0.329	0.327	0.326	0.363	0.223	0.205	0.202	0.199	0.203
0.4	0.409	0.437	0.433	0.432	0.454	0.195	0.182	0.193	0.178	0.181
0.5	0.507	0.539	0.535	0.534	0.541	0.165	0.157	0.180	0.155	0.157
0.6	0.605	0.638	0.633	0.632	0.627	0.135	0.131	0.163	0.129	0.131
0.7	0.702	0.732	0.729	0.727	0.717	0.103	0.103	0.139	0.101	0.102
0.8	0.801	0.824	0.824	0.82	0.81	0.071	0.071	0.107	0.071	0.071
0.9	0.899	0.917	0.919	0.914	0.908	0.036	0.037	0.062	0.037	0.037
	1050 K									
x_{Sn}	a_{Sn}					a_{Ga}				
0.1	0.103	0.105	0.104	0.105	0.105	0.291	0.264	0.227	0.257	0.257
0.2	0.206	0.211	0.253	0.212	0.212	0.262	0.237	0.219	0.232	0.233
0.3	0.307	0.316	0.349	0.319	0.317	0.231	0.211	0.209	0.208	0.209
0.4	0.406	0.421	0.440	0.424	0.421	0.199	0.185	0.196	0.183	0.185
0.5	0.505	0.523	0.528	0.526	0.522	0.167	0.157	0.179	0.156	0.158
0.6	0.604	0.622	0.617	0.625	0.621	0.135	0.129	0.159	0.129	0.131
0.7	0.703	0.720	0.709	0.722	0.718	0.102	0.098	0.132	0.099	0.101
0.8	0.802	0.817	0.804	0.817	0.814	0.069	0.068	0.099	0.068	0.069
0.9	0.902	0.914	0.904	0.913	0.910	0.035	0.035	0.057	0.035	0.036

Table 6 Continued

Alloy	Chou	Toop	Hillert	Kohler	Muggianu	Chou	Toop	Hillert	Kohler	Muggianu
	1100 K									
x_{Sn}	a_{Sn}					a_{Ga}				
0.1	0.102	0.101	0.134	0.103	0.103	0.287	0.278	0.240	0.272	0.272
0.2	0.203	0.204	0.243	0.207	0.207	0.256	0.248	0.229	0.243	0.244
0.3	0.304	0.307	0.338	0.310	0.309	0.225	0.218	0.215	0.215	0.216
0.4	0.404	0.409	0.429	0.413	0.411	0.193	0.188	0.198	0.187	0.188
0.5	0.504	0.512	0.517	0.514	0.512	0.162	0.157	0.178	0.158	0.159
0.6	0.604	0.612	0.608	0.614	0.617	0.129	0.127	0.155	0.128	0.129
0.7	0.704	0.712	0.701	0.713	0.710	0.098	0.096	0.126	0.098	0.098
0.8	0.804	0.811	0.798	0.811	0.808	0.065	0.064	0.093	0.066	0.067
0.9	0.903	0.909	0.899	0.909	0.907	0.033	0.032	0.052	0.033	0.034

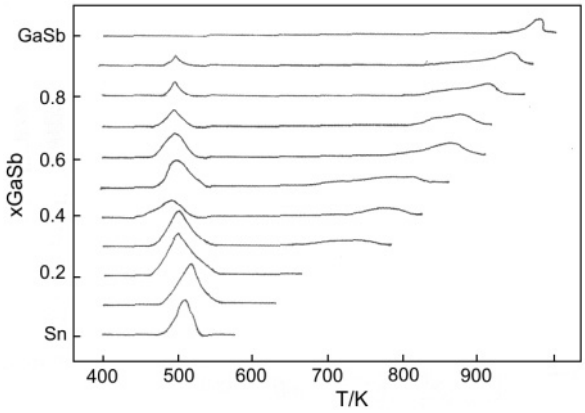

Fig. 5 DTA curves obtained for the investigated Ga–Sb–Sn alloys

Fig. 6 Characteristic microphotograph for sample L6 (magnification ‡ 120×) (light phase – primary solidified GaSb crystals; dark phase – binary eutectics (GaSb–Sn))

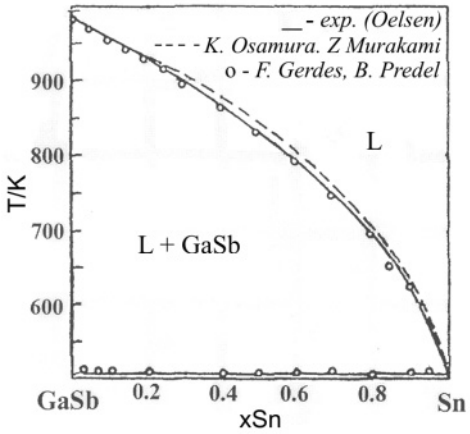

Fig. 7 Phase diagram of the GaSb–Sn system

Good agreement was noticed between results of experimental research, presented in this work, and literature data [20, 21].

Conclusions

The thermodynamic properties of the GaSb-Sn system were experimentally (Oelsen calorimetry, EMF measurements with zirconia as solid electrolyte) and analytically (thermodynamic predicting methods: Chou's general solution model, Toop, Kohler, Muggianu, Hillert) determined. The calculated results show agreement between data obtained by different models, as well as with experimental data. Phase diagram investigation confirmed good agreement between experimental research (DTA, optical microscopy) and literature data for the investigated Bi–GaSb system.

Obtained results could be useful in further interpretation of the phenomena occurring in the ternary Ga–Sb–Sn system and in the compilation of the thermodynamic studies of III–V compounds-related materials at high temperatures.

References

1 I. Katayama, J. I. Nakayama, T. Ikura, Z. Kozuka and T. Iida, Mat. Trans. JIM, 34 (1993) 792.
2 I. Katayama, J. I. Nakayama, T. Ikura, T. Tanaka, Z. Kozuka and T. Iida, J. Non-Cryst. Sol., 156–158 (1993) 393.
3 J. Šestak, V. Šestakova, Ž. Živković and D. Živković, Pure and Appl. Chem., 67 (1995) 1885.
4 I. Katayama, T. Ikura, K. Maki and T. Iida, Mat. Trans. JIM, 36 (1995) 41.
5 D. Živković, Ž. Živković, L. Stuparević and S. Ranić, J. Therm. Anal. Cal., 65 (2001) 805.
6 L. Kaufman, J. Nell, K. Taylor and F. Hayes, CALPHAD, 5 (1981) 185.
7 I. Katayama, J. Nakayama, T. Nakai and Z. Kozuka, Trans. JIM, 28 (1987) 129.
8 C. Bergman, M. Laffite and Y. Muggianu, High Temp.- High Press, 6 (1974) 53.
9 T. J. Anderson, T. L. Aselage and L. F. Donaghey, J. Chem. Thermodyn., 15 (1983) 927.
10 T. Aselage, K. M. Chang and T. J. Anderson, CALPHAD, 9 (1985) 227.
11 R. C. Sharma, T. L. Ngai and Y. A. Chang, J. Electron. Mater., 16 (1987) 307.
12 I. A. Merzhanov, V. A. Geiderikh and V. I. Goryacheva., Zh. Fiz. Khim., 49 (1985) 874.
13 S. Ravindra Reddy and J. P. Hajra, Mater. Sci. Eng., B20 (1993) 308.
14 R. Hultgren, P. D. Desai, D. T. Hawkins, M. Gleiser and K. Kelley, The Selected Values of the Thermodynamic Properties of Binary Alloys, ASM, Metals Park, OH, 1973.
15 I. Katayama, K. Maki, M. Nakano and T. Iida, Mat.Trans. JIM, 37 (1996) 988.
16 V. N. Danilin and S. P. Yatsenko, Izv. Akad. Nauk SSSR, Metall, 5 (1968) 14.
17 J. Anderson and I. Ansara, J. Phase Equilib., 13 (1992) 181.
18 B. Predel, J. Less-Common Met., 7 (1964) 347.
19 I. Katayama, Y. Fukuda, Y. Hattori and T. Maruyama, Thermochim. Acta, 314 (1998) 175.
20 K. Osamura and Y. Murakami, J. Phys. Chem. Solids, 36 (1975) 931.
21 F. Gerdes and B. Predel, J. Less-Common Met., 79 (1981) 281.
22 W. Oelsen and P. Zuhlke, Arch. Eisenhuttenwessen, 27 (1956) 743.
23 W. Oelsen, E. Schurmann, H. J. Weigt and O. Oelsen, Arch. Eisenhuttenwessen, 27 (1956) 487.
24 W. Oelsen, F. Bieret and G. Schwabe, Arch. Eisenhuttenwessen, 27 (1956) 607.
25 K. C. Chou, CALPHAD, 19 (1995) 315.
26 K. C. Chou, W. C. Li, F. Li and M. He, CALPHAD, 20 (1996) 395.

27 G. W. Toop, Trans. Met. Soc. AIME, 233 (1965) 850.
28 F. Kohler, Monatsh. Chem., 91 (1960) 738.
29 Y. M. Muggianu, M. Gambino and J. P. Bross, J. Chimie Physique, 72 (1975) 83.
30 M. Hillert, CALPHAD, 4 (1980) 1.